Molecular Crystals and Liquid Crystals

Publication details, including instructions for authors and subscription information:
http://www.tandfonline.com/loi/gmcl20

Micro-Photopatterning with Photo-Decomposable Polymer Langmuir-Blodgett (LB) Films

Tiesheng Li [a b], Guoliang Zeng [a b], Suhua Zhang [a b], Wenjian Xu [a b] & Yangjie Wu [a b]

[a] Department of Chemistry, Zhengzhou University, Henan Key Laboratory of Chemistry, Biology, and Organic Chemistry, Zhengzhou, China

[b] and Key Lab of Advanced Information Nano-Materials of Zhengzhou, Zhengzhou, China

Version of record first published: 22 Sep 2010

To cite this article: Tiesheng Li, Guoliang Zeng, Suhua Zhang, Wenjian Xu & Yangjie Wu (2008): Micro-Photopatterning with Photo-Decomposable Polymer Langmuir-Blodgett (LB) Films, Molecular Crystals and Liquid Crystals, 490:1, 67-79

To link to this article: http://dx.doi.org/10.1080/15421400802305848

Mol. Cryst. Liq. Cryst., Vol. 490, pp. 67–79, 2008

ISSN: 1542-1406 print/1563-5287 online
DOI: 10.1080/15421400802305848

Micro-Photopatterning with Photo-Decomposable Polymer Langmuir–Blodgett (LB) Films

Tiesheng Li, Guoliang Zeng, Suhua Zhang, Wenjian Xu, and Yangjie Wu
Department of Chemistry, Zhengzhou University, Henan Key Laboratory of Chemistry, Biology, and Organic Chemistry, Zhengzhou, China, and Key Lab of Advanced Information Nano-Materials of Zhengzhou, Zhengzhou, China

A new series of copolymer [Poly(N-hexadecylmethacrylamide-co-4-tert-butylphenl methacrylate)s] (p(HDMA–BPhMA)s) which contain N-hexadecylmeth- acrylamide (HDMA) and 4-tert-butylphenl methacrylate (BPhMA) was synthesized. The monolayer behavior of p(HDMA–BPhMA)s with different mole fraction of BphMA on the water surface was investigated. The copolymer (p(HDMA–BPhMA)s) which contains a low mole fraction of BPhMA could form a stable, condensed monolayer and could be transferred to solid substrates giving Y-type Langmuir–Blodgett (LB) films. The photopatteming properties and decompose mechanism of p(HDMA–BPhMA) LB films irradiated by deep UV light is that the scission of the main chain and the side chain occurred from the results of IR, UV spectra, and GPC measurement. A resolution (0.75 μm) of p(HDMA–BPhMA30) LB films irradiated by deep UV light, followed by development with acetone was obtained. The p(HDMA–BPhMA30) LB films also show a high resistance ability and high aspect ratio in the proceed of etching gold and copper film. The morphological investigation of the pattern on the mica substrate was carried out by atom force microscopy (AFM).

Keywords: etching; Langmuir–Blodgett films; photolithography; polymer

1. INTRODUCTION

Lithographic technology is based on projecting an optical image of a device onto a resist in order to record the image for subsequent processing steps [1]. With the development of the integrate circuit chip

Address correspondence to Tiesheng Li, Department of Chemistry, Zhengzhou University, Henan Key Laboratory of Chemistry, Biology, and Organic Chemistry, Zhengzhou 450052, China. E-mail: lts34@zzu.edu.cn

technology. Much attention has been paid to the high resolution photolithography technology and exploring high sensitive resist. The resolution is limited by resist materials and light source [2] in the resist development processes. Moreover, the thickness of the resist film is also a main factor to limit the resolution [3]. LB films which have ordered structure and controllability of film thickness on the order of molecular sizes have attractive features [4–6]. They cannot only overcome the weakness of spin-coat films, in which molecules are distributed randomly, but also be expected to improve the resolution and the sensitivity of the resist effectively [7,8]. Many researches were reported on fine-pattern drawing using LB films such as G. Wegner *et al.* synthesized the polyglutamate derivatives and obtained the negative pattern [9], Ringsdorf *et al.* studied photopolymerization of octadiene- and docosadiene-derivative LB films [10]. M. Crooks and Atsushi Aoki investigated fine pattern of hyperbranched poly(tert-butyl acrylate) by UV irradiation [11]. The group of Tokuji Miyashita made a great progress in studying the photolithographic materials with a series of LB films containing N-alkyl acrylamide. They yielded the fine negative-tone patterns using N-alkylmethacrylamide monomers [7,8] or cross-linkable polymer LB films [12,13] irradiated by EB beam or UV light. Moreover, the fine positive-tone patterns were also obtained using the copolymer of t-butyl 4-vinylphenyl carbonate (tBVPC) and different N-alkyl methacrylamide [14–16]. The copolymer LB films containing anthracene moieties [17] and the homopolymer LB films with short-branched alkyl side chains [18] were also investigated for photopatterning.

In previous studies, many investigations were concentrated on how to transfer patterns to substrates by LB films technology. But the morphological of the transferred patterns on the substrates were not studied. In this article, we prepared a new series of new *diblock* copolymers (p(HDMA–BPhMA)s) which composed of N-hexadecylmethacrylamide (HDMA) and 4-tert-butylphenl methacrylate (BPhMA), in which HDMA has an excellent ability to form stable monolayer on water surface [7], and the carbonyl ester of BPhMA can be decomposited by deep UV irradiation. The copolymer was prepared to LB films, which have a good sensitivity and high resistance ability. The mechanism of the pattern formation was also investigated. Moreover, the morphological of the pattern transferred to substrate was studied by AFM.

2. EXPERIMENTAL

2.1. Materials

HDMA was synthesized by reaction of methylacryloyl chloride with hexadecylamine in the presence of triethylamine in chloroform and

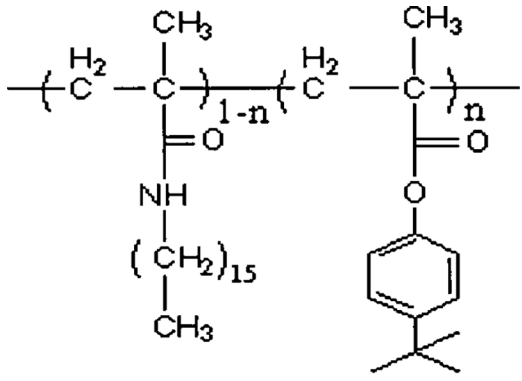

p(HDMA-BPhMA)s

FIGURE 1 Chemical structure of p(HDMA–BPhMA)s.

purified by chromatography. BPhMA was synthesized by reaction of methylacryloyl chloride with the 4-tert-butylphenol in the presence of triethylamine in chloroform and purified by chromatography. The copolymers p(HDMA–BPhMA)s shown in Fig. 1 were prepared by free-radical polymerization of HDMA and BPhMA in dried benzene at 75°C, with AIBN as a thermal initiator under N_2 atmosphere for about 20 h [19,20]. The copolymers were purified by dissolution in chloroform, filtering, and precipitation with a large excess of ethanol twice, and dried under vacuum at room temperature. The copolymer compositions were determined by the integrated intensity of characteristic signals of each monomer in the ^{1}H NMR spectra. The properties of the copolymers are summarized in Table 1.

TABLE 1 Characteristics of p(HDMA–BPhMA)s.

Polymer and Copolymer	pBPhMA in feed (mol%)	BPhMA mol%	Mn (10^4)	Mw (10^4)	Mn/Mw	Yield wt.%
pBPhMA	100.0	100.0	1.33	2.60	1.96	25.0
pHDMA–BPhMA71	50.0	71.32	2.53	4.53	1.79	24.0
pHDMA–BPhMA53	33.3	53.27	2.23	6.64	2.98	62.5
pHDMA–BPhMA30	20.0	29.70	1.30	2.77	2.13	35.0
pHDMA–BPhMA19	11.1	19.34	1.29	1.92	1.49	41.3
pHDMA–BPhMA12	6.3	12.50	1.38	3.92	2.83	54.9
pHDMA–BPhMA7	4.7	6.67	0.94	1.15	1.23	57.8

2.2. Measurements

^{1}H NMR spectra were obtained in $CDCl_3$ with tetramethylsilane (TMS) as an internal standard Bruker DPX-400 spectrometer. Molecular weight was measured with gel permeation chromatography GPC50 (PL) using a polystyrene as a standard. UV measurement was carried out with a Lambda 35 UV-vis spectrophotometer. FT-IR spectra were measured with a Bruker VECTOR 22 spectrometer. The optical exposures were performed with a deep UV lamp (EX250, HOYA); gold and copper film on the glass substrate was sputtered by Bench Top Turbo IV Coating System. The patterns were observed by OLYMPUS BX51 microscopy. Consistent force mode AFM image was obtained using a SPM-9500 J3 atomic force microscopy at ambient.

2.3. Monolayer and Multilayer Formation

Measurement of surface pressure (π)-surface area (A) isotherms and the deposition of monolayer were carried out with a computer controlled Langmuir trough (KSV 5000-3) at a compression speed of $10\,cm^2$/min at 25°C. The deposition was performed both up and down strokes at a speed of 10 mm/min. Deionized pure water (Milli-Q II MILLIPORE, $18.2\,M\Omega \cdot cm$) was used as the subphase. The copolymer was spread on the water surface from a very diluted solution (0.54 mg/ml) in chloroform, and the solvent was allowed to evaporate. Quartz, glass, and silicon slides to be used for LB film were prepared by treating with boiling concentrated HNO_3 solution, then washing with water, reacting with trichlorooctadecylsilane to make it hydrophobic.

3. RESULTS AND DISCUSSION

3.1. Monolayer Behavior on the Water Surface and LB Films Formation

Figure 2 showed π-A isotherms of p(HDMA–BPhMA)s monolayer with different mole fraction of BPhMA at 25°C. It was clear that the isotherms varied according to the mole fraction of BPhMA. The π-A isotherms of **a, b, c,** and **d** showed sharp rise in surface pressure and high collapse pressure, suggesting that the condensed monolayer was formed on the water surface. The π-A isotherms of **e, f,** and **g** showed slow rise in surface pressure and low collapse pressure, which indicated that an expanded monolayer was formed on the water surface. The copolymer p(HDMA–BPhMA) which contained a low mole fraction of BPhMA could form a stable, condensed monolayer on the water surface.

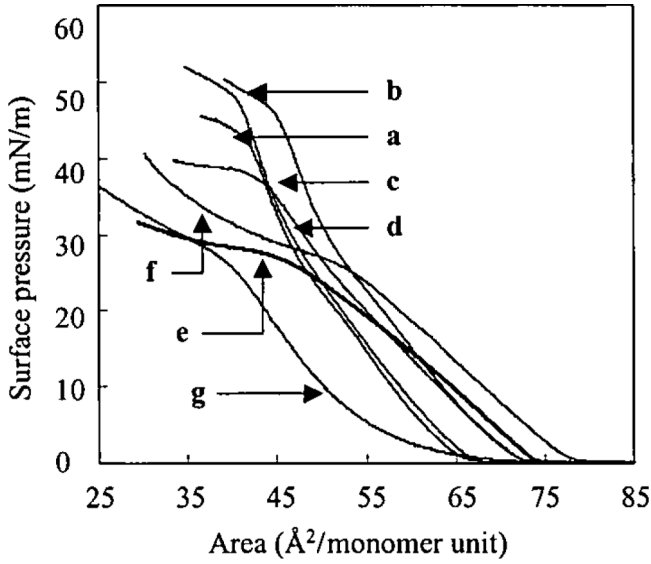

FIGURE 2 Surface pressure (π)-surface area (A) isotherms of p(HDMA–BPhMA)s; **a,** p(HDMA–BPhMA7); **b,** p(HDMA–BPhMA12); **c,** p(HDMA–BPhMA19); **d,** p(HDMA–BPhMA30); **e,** p(HDMA–BPhMA53); **f,** p(HDMA–BphMA71); **g,** pBPhMA.

The monolayers of **a, b, c,** and **d** could be transferred onto solid supports as a Y-type LB films under a given surface pressure with the transfer ratio which is almost unity. The UV spectra of p(HDMA–BPhMA30) LB films (deposited under 30 mN/m) were measured as a function of the number of deposited layers (Fig. 3). The intensity of maximal absorbance at 193 nm was proportional to the number of layers. It indicated that the regular homogeneous deposition occurred.

3.2. Photopatterning

The copolymers [p(HDMA–BPhMA7), p(HDMA–BPhMA12), p(HDMA–BPhMA19), and p(HDMA–BPhMA30)] LB films of 40 layers were irradiated by deep UV lamp ($\lambda = 250$ nm) through a photomask for 20 min in the air and developed with 1% tetramethylammonium hydroxide (TMAH) aqueous solution or acetone. p(HDMA–BPhMA30) LB films gave the finest patterns (Fig. 4) with the resolution of 0.75 μm linewidth, which is the limit of the photomask employed. Compared to developing by TMAH aqueous solution, acetone was more convenience

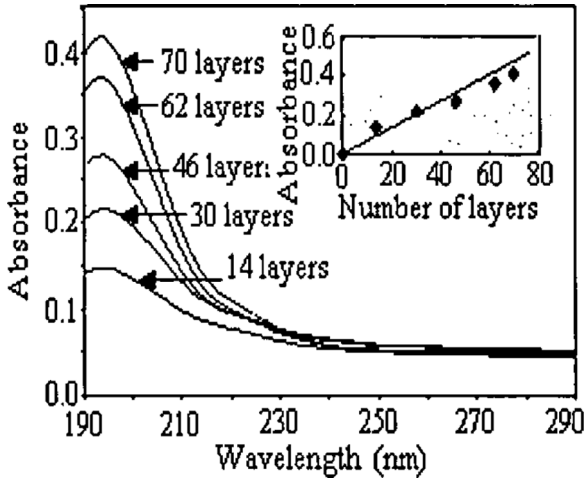

FIGURE 3 UV spectra of p(HDMA–BPhMA30) LB films as a function of the number of layers deposited. Inset: Linear relationship between the maximal absorbance at 193 nm and the number of deposited layers.

to be employed. Therefore, the subsequent experiments for photopatterning were carried out with p(HDMA–BPhMA30) LB films and developed by acetone.

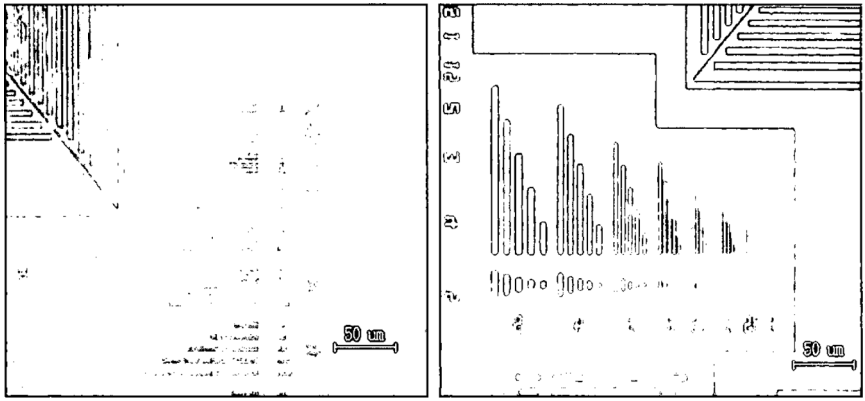

(a) (b)

FIGURE 4 Optical micrograph of positive patterns with p(HDMA–BPhMA30) LB films (40 layers) on silicon wafer irradiated by deep UV lamp for 20 min, followed by the development with (a) 1% TMAH aqueous solution for 20 s, (b) acetone for 10 s.

3.3. Photo-Decomposing Mechanism of the Copolymer LB Films

The photopatterning mechanism was studied by UV spectra, gel permeation chromatography (GPC) measurement, and FT-IR spectra. Figure 5 was the UV spectra change of 80 layers of p(HDMA–BPhMA30) LB films irradiated by deep UV lamp ($\lambda = 250$ nm) directly. The absorption band at 193 nm was assigned to back bone decreased sharply as the UV irradiation proceeded and almost disappeared at last. This indicated that the scission of back bone occurred. Besides, the absorbance decreased sharply in a short time, which indicated that the LB films of p(HDMA–BPhMA30) were sensitive to the UV light.

In order to confirm whether the scission of back bone really happened or not during the UV irradiation, the GPC measurement was carried out. Because the amount of the LB films was too small, the measurement had to be carried out with the spin-coat films which was transferred in THF after irradation. As show in Fig. 6, the molecular weight of p(HDMA–BPhMA30) apparently decreased under the deep UV irradiation ($\lambda = 250$ nm), which indicated that the scission of back bone of the copolymer took place.

Figure 7 showed FT-IR spectra change of 120 layers of p(HDMA–BPhMA30) LB films, which were deposited on the CaF_2 substrate,

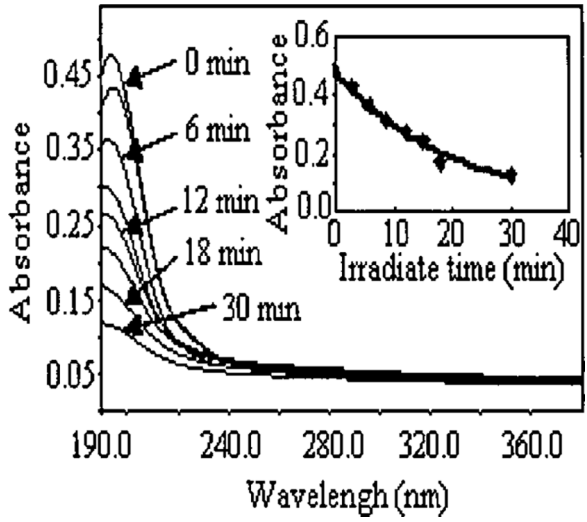

FIGURE 5 Changes of UV spectra of p(HDMA–BPhMA30) LB films of 80 layers deposited on the quartz substrate. Inset: relationship between the irradiated time and the maximal absorbance at 193 nm.

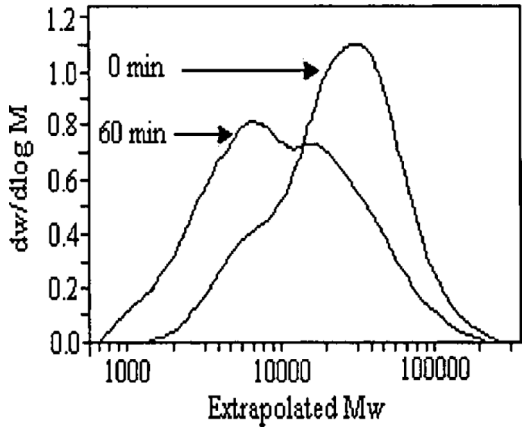

FIGURE 6 Molecular weight change of p(HDMA–BPhMA30) spin-coat films under the deep UV irradiation.

irradiated by deep UV lamp. The peak at 1170 cm^{-1} assigned to C–O stretching vibration of the ester and the carbonyl ester band at 1745 cm^{-1} disappeared after UV irradiation. Meanwhile, another peak which assigned to the carbonyl group of the −COOH could be observed

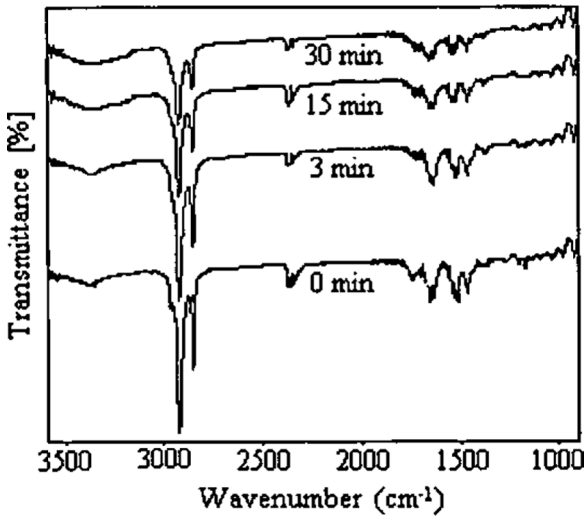

FIGURE 7 Change of IR spectra of 120 layers of p(HDMA–BPhMA30) LB films, which were deposited on CaF_2 substrate, irradiated by deep UV light for 0, 3, 15, and 30 min.

at 1718 cm^{-1}; these indicated that the ester was decomposed and −COOH was produced. It could also be confirmed by the fact that the intensity of the peak at 3360 cm^{-1} significantly increased and broadened, which means the hydroxyl group was produced. Moreover, the absorbance at 2923 cm^{-1} assigned to the alkyl group decreased dramatically after UV irradiation. This change also confirmed the scission of side chain in the copolymer, and it was the main reason that the pattern can be developed by acetone.

3.4. Etching Properties

The resistance ability of p(HDMA–BPhMA30) LB films was also studied. The p(HDMA–JBPhMA30) LB films with 20, 40, 60 layers were deposited on the gold film which was sputtered on glass substrate and were irradiated through a photomask for 10, 20, 30 min, respectively, then developed by acetone for 5, 10, 20 s, respectively. The positive-tone patterns were immersing to a mixed solution which consisted of iodide (0.6 g), ammonium iodide (1.5 g), ethanol (20 ml), and water (30 ml) for 20 s. Finally, the p(HDMA–BPhMA30) LB films were removed by chloroform for 20 s. The LB films with 40 and 60 layers showed excellent resistance ability, but the resolution of the LB films with 40 layers [Fig. 8(a)] was 0.75 μm, which was better than the resolution of LB films with 60 layers.

The positive-tone patterns (40 layers) on the copper film were also investigated; they were etched by enchant which consisted of $CuCl_2$ (2.13 g), NH_4Cl (0.319 g), H_2O (4.0 ml) for 4–5 min at 50°C [21], and the residual films were removed by chloroform; the fine patterns could

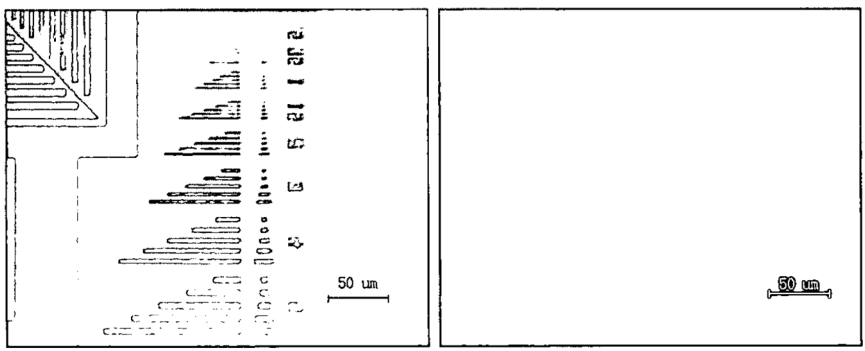

(a) (b)

FIGURE 8 (a) Etched pattern of gold film on the glass substrate, (b) Etched pattern of copper film on the glass substrate.

also be obtained with the resolution of 0.75 μm [Fig. 8(b)]. These indicated that the p(HDMA–BPhMA30) LB films as nanomaterials showed high resistance to wet etching because of their high, densely packed structure.

3.5. Morphological Study of the Patterns

The morphology of the pattern was studied by AFM. Figure 9 showed the AFM image of the patterns transferred to the LB films. The average height of the lines which was more than 2 μm wide was 55 nm, the height of the 1.2 μm wide lines and 0.75 μm line width was 49.63, 30.09 nm, respectively (Figs. 9(c) and 9(d)). The height of the lines decreased apparently as the width of the lines decreased.

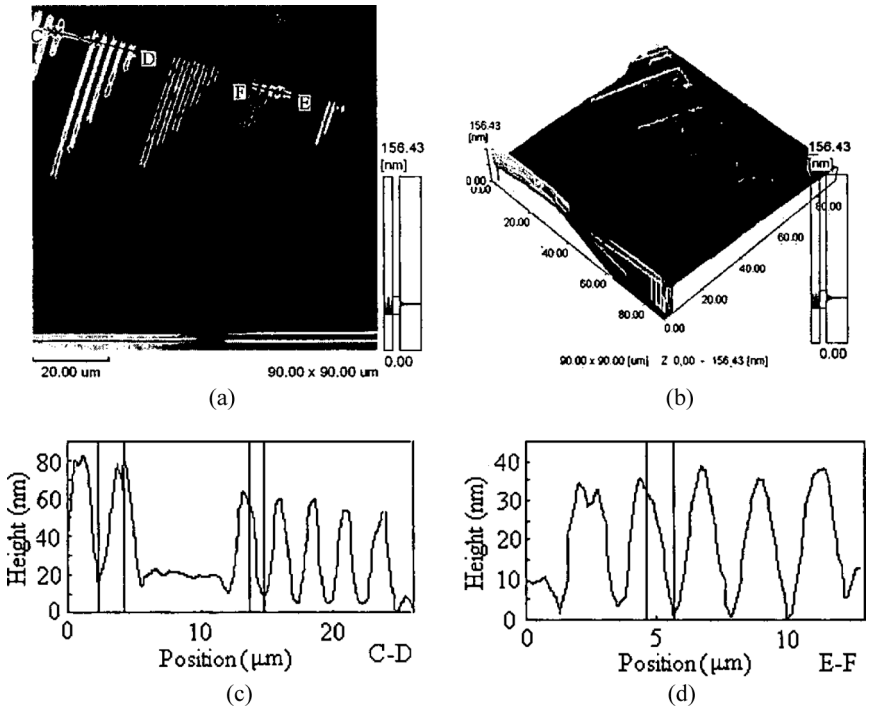

FIGURE 9 AFM images of LB films pattern on gold film coated on mica substrate (bright area of the patterns correspond to patterns of LB films, while the brown regions correspond to gold films): (a) surface image of patterns of p(HDMA–BPhMA30) LB films; (b) 3-D image of a; section analysis image: (c) cross-sectional profile of resolution is 2 (lift) and 1.2 μm (right) line width; (d) cross-sectional profile of resolution is 0.75 μm line width.

This should be caused by the unsatisfactory contact between the film surface and the mask during the photo-patterning process, and the diffraction occurred when the UV light went through the narrow slits between the lines. The diffraction affected the pattern transformation apparently especially on the lines which had higher resolution. Consequently, the regions of the films should not have been irradiated because the coverage of the mask was also irradiated slightly by UV light, so the films were dissolved partly in the development process, and the height decreased. The lines which were more than 2 μm wide had the same height (55 nm), which indicated the effect of diffraction on these lines was negligible, and 55 nm could be regarded as the total height of the LB films with 40 layers. Therefore, the thickness of each deposition layer in the films was 1.37 nm.

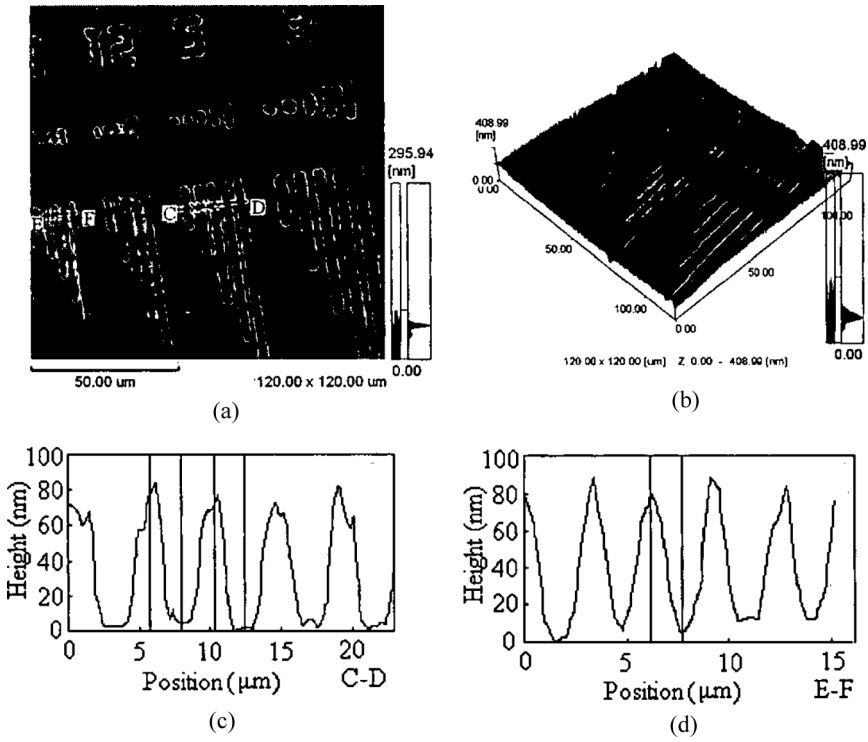

FIGURE 10 AFM image of gold pattern on mica substrate (bright area corresponds to surface of mica, while the brown regions correspond to the patterns of gold films): (a) surface image of gold patterns on mica; (b) 3D AFM image of a; (c) section image with the resolution of 2 μm line width; (d) section image with the resolution of 1 μm line width.

After removing the p(HDMA–BPhMA30) LB films on the gold film, the gold pattern was studied by AFM as show in Fig. 10. According to the section image, the heights of gold lines with different resolution were almost the same (73.30, 72.08, 72.88 nm) (Figs. 10(c) and 10(d)), so the average height of the gold film was 73 nm. Although the p(HDMA–BPhMA30) LB films of the minimal line width after irradiation were dissolved partly in the development process, the residual layers also had enough resist ability against enchant in the wet etching process. It indicated that the p(HDMA–BPhMA30) LB films had a high resistance to the wet enchant. The sidewalls of gold lines were not vertical to substrate perfectly, and the width of the top of the gold lines was much smaller than that in the bottom. The reason was that the etching was non-orientation, the enchant not only etched the gold film vertical to the substrate, but also etched on the parallel orientation of the substrate simultaneously. This effect was much more apparent to the lines which have high resolution.

4. CONCLUSION

The copolymer p(HDMA–BPhMA)s with different mole fraction of BPhMA were synthesized and characterized by ^{1}H NMR spectra and GPC measurement. The p(HDMA–BPhMA)s with low mole fraction of BPhMA were much easier to form condensed monolayer than those *with high mole fraction* on the water/air interface, and they could be transferred to solid substrates. p(HDMA–BPhMA30) LB films on the silicon substrate irradiated by UV light and developed by acetone yielded a fine pattern with the resolution of 0.75 μm, which was the limit resolution of the photomask employed. The formation of the pattern was due to the scission of the main chain and the cleavage of the side chain. The resistance ability of p(HDMA–BPhMA30) LB films was also studied, and the LB films with 40 layers showed good resistance ability; the minimal gold and copper line width of 0.75 μm on glass substrate were obtained. AFM studies also showed that p(HDMA–BPhMA30) LB films had high resistance ability in the photolithography process. The photopatterning properties and high resistance ability of p(HDMA–BPhMA) LB films are expected to be applied as a new photoresist material.

ACKNOWLEDGMENTS

The authors thank prof. Luyuan Mao and Afang Zhang, College of Materials Science and Engineering, Zhengzhou University, for the use of AFM and GPC instrument. This work is partially supported

by The Innovation Fund for Outstanding Scholar of Henan Province (0621001100); The Fund for Outstanding Younger Scholar of Henan Province (074100510015); The Nature Science Foundation of China (20572102); The Scientific Research Foundation for the Returned Chinese Scholar, State Education Ministry, and The Personnel Department of Henan Province; and Nature Science Foundation of Henan Province (0611020100).

REFERENCES

[1] Brainard, R. L., Barclay, G. G., Anderson, E. H., & Ocola, L. E. (2002). *Microelectronic Engineering*, *61–62*, 707.
[2] Shibayama, K. & Kato, T. (1986). *Polymer Engineering and Science*, *26*, 1140.
[3] Steitz, R., Mitchell, E. E., & Peterson, I. R. (1991). *Thin Solid Films*, *205*, 124.
[4] Mizuta, Y., Matsuda, M., & Miyashita, T. (1993). *Langmuir*, *9*, 1110.
[5] Miyashita, T. & Ito, Y. (1995). *Thin Solid Films*, *260*, 217.
[6] Lu, Q. & Liu, M. H. (2003). *Thin Solid Films*, *425*, 248.
[7] Guo, Y. Z., Feng, F., & Miyashita, T. (1999). *Macromolecules*, *32*, 1115.
[8] Li, X. D., Aoki, A., & Miyashita, T. (1997). *Macromolecules*, *30*, 2194.
[9] Mathauer, K., Schmidt, A., Knoll, W., & Wegner, G. (1995). *Macromolecules*, *28*, 1214.
[10] Laschewsky, A. & Ringsdorf, H. (1988). *Macromolecules*, *21*, 1936.
[11] Aoki, A., Ghosh, P., & Crooks, R. M. (1999). *Langmuir*, *15*, 7418.
[12] Miyashita, T., Nakaya, M., & Aoki, A. (1998). *Supramolecular Science*, *5*, 3.
[13] Aoki, A. & Miyashita, T. (2001). *Polymer*, *42*, 7307.
[14] Li, T. S., Misuishi, M., & Miyashita, T. (2001). *Thin Solid Films*, *389*, 267.
[15] Li, T. S., Mitsubishi, M., & Miyashita, T. (2004). *Thin Solid Films*, *446*, 138.
[16] Li, T. S., Mitsubishi, M., & Miyashita, T. (2005). *Advances in Technology of Materials and Materials Processing*, *7*, 209.
[17] Li, T. S., Chen, J. F., Mitsubishi, M., & Miyashita, T. (2003). *Journal of Materials Chemistry*, *13*, 1565.
[18] Guo, Y. Z., Mitsubishi, M., & Miyashita, T. (2001). *Macromolecules*, *34*, 3548.
[19] Bresler, S. E., Sheremeteva, T. V., Frenkel, S. Ya., & Zhenevskaya, M. G. (1957). *Inst. Macromol. Compds. Leningrad, Zhur. Fiz. Khim.*, *31*, 109.
[20] Filipovic, J. M., Petrovic-Dakov, D. M., & Vrhovac, L. P. (1992). *Journal of Thermal Analysis*, *38*, 709.
[21] Cakir, O. (2006). *Journal of Materials Processing Technology*, *175*, 63.